Supporting Information

Luminescence switch-on assay of interferon-gamma using a G-quadruplex-selective iridium(III) complex

Sheng Lin,[a] Bingyong He,[a] Chao Yang,[b] Chung-Hang Leung,[b,*] Jean-Louis Mergny[c,d,*] and Dik-Lung Ma[a,e,*]

[a] *Department of Chemistry, Hong Kong Baptist University, Kowloon Tong, Hong Kong, China. Email: edmondma@hkbu.edu.hk*
[b] *State Key Laboratory of Quality Research in Chinese Medicine, Institute of Chinese Medical Sciences, University of Macau, Macao, China. Email: duncanleung@umac.mo*
[c] *University of Bordeaux, ARNA laboratory, Bordeaux, France. Email: jean-louis.mergny@inserm.fr*
[d] *INSERM, U869, IECB, Pessac, France.*
[e] *Partner State Key Laboratory of Environmental and Biological Analysis, Hong Kong Baptist University, Kowloon Tong, Hong Kong, China.*

Materials

Reagents, unless specified, were purchased from Sigma-Aldrich (St. Louis, MO, USA) and used as received. Iridium chloride hydrate ($IrCl_3 \cdot xH_2O$) was purchased from Precious Metals Online (Australia). Interferon-gamma (IFN-γ) was purchased from Sino Biological Inc. (China). Calf thymus DNA (ct-DNA, 42% GC and 58% AT) was purchased from Sigma-Aldrich (St Louis, MO, USA) and purified by the literature method.[1] The concentration was determined by ultraviolet absorbance measurements using the extinction coefficient: ε260 = 12824 $M^{-1} \cdot cm^{-1}$. [1] All other oligonucleotides were synthesized by Techdragon Inc. (Hong Kong, China).

DNA sequences used in this project:

ssDNA: 5'-$C_2AGT_2CGTAGTA_2C_3$-3',

ds26: 5'-$CA_2TCG_2ATCGA_2T_2CGATC_2GAT_2G$-3',

c-kit87: 5'-$AG_3AG_3CGCTG_3AG_2AG_3$-3',

Pu22: 5'-$TGAG_3TG_4AG_3TG_4A_2$-3',

CCR5: 5'-$CTCAT_4C_2ATACAT_2A_3GATAGTCAT$-3',[2]

D: 5'-$TG_4T_2G_2T_2GT\ GT_2G_3TGT_2GTGTATC_3TC_2GCG$-3',

L: 5'-$G_3AG_2AG_3TCGCG_3AG_3ATC_2ACA_2C_2A_2C_4A$-3',

L-mutant: 5'- $GAGAG_2AGTGTCGCGCGAGTGATC_2ACA_2C_2A_2C_4A$-3'.

General experimental

Mass spectrometry was performed at the Mass Spectroscopy Unit at the Department of Chemistry, Hong Kong Baptist University, Hong Kong (China). Deuterated solvents for NMR purposes were obtained from Armar and used as received. ^{1}H and ^{13}C NMR were recorded on a Bruker Avance 400 spectrometer operating at 400 MHz (^{1}H) and 100 MHz (^{13}C). ^{1}H and ^{13}C chemical shifts were referenced internally to solvent shift (CD_3CN: ^{1}H, δ 1.94, 13C, δ 118.7; d_6-DMSO: 1H, δ 2.50, 13C, δ 39.5). Chemical shifts (δ) are quoted in ppm, the downfield direction being defined as positive. Uncertainties in chemical shifts are typically ±0.01 ppm for ^{1}H and ±0.05 for ^{13}C. Coupling constants are typically ± 0.1 Hz for ^{1}H-^{1}H and ±0.5 Hz for ^{1}H-^{13}C couplings. The following abbreviations are used for convenience in reporting the multiplicity of NMR resonances: s, singlet; d, doublet; t, triplet; q, quartet; m, multiplet; br, broad. All NMR data was acquired and processed using standard Bruker software (Topspin).

Photophysical measurement

Emission spectra and lifetime measurements for complexes were performed on a PTI TimeMaster C720 Spectrometer (Nitrogen laser: pulse output 337 nm) fitted with a 380 nm filter. Error limits were estimated: λ (±1 nm); τ (±10%); φ (±10%). All solvents used for the lifetime measurements were degassed using three cycles of freeze-vac-thaw.

Luminescence quantum yields were determined using the method of Demas and Crosby[3] $[Ru(bpy)_3][PF_6]_2$ in degassed acetonitrile as a standard reference solution (Φ_r = 0.062) and calculated according to the following equation:

$$\Phi_s = \Phi_r(B_r/B_s)(n_s/n_r)^2(D_s/D_r)$$

where the subscripts s and r refer to sample and reference standard solution respectively, n is the refractive index of the solvents, D is the integrated intensity, and Φ is the luminescence quantum yield. The quantity B was calculated by $B = 1 - 10^{-AL}$, where A is the absorbance at the excitation wavelength and L is the optical path length.

Luminescence response of complexes towards different forms of DNA

The G-quadruplex DNA-forming sequences were annealed in Tris-HCl buffer (10 mM Tris, 20 mM KCl, pH 7.2) and were stored at –20 °C before use. Complex (1.0 μM) was added to 5 μM of ssDNA, dsDNA or G-quadruplex DNA in Tris-HCl buffer (10 mM Tris, pH 7.2).

Fluorescence resonance energy transfer (FRET) melting assay

The ability of **8** to stabilize G-quadruplex DNA was investigated using a fluorescence resonance energy transfer (FRET) melting assay. The labelled G-quadruplex-forming oligonucleotide F21T (5′-*FAM*-d($G_3[T_2AG_3]_3$)-*TAMRA*-3′; donor fluorophore FAM: 6-carboxyfluorescein; acceptor fluorophore TAMRA: 6-carboxytetramethylrhodamine) was diluted to 200 nM in a potassium cacodylate buffer (100 mM KCl, pH 7.0), and then heated to 95 °C in the presence of the indicated concentrations of **8**. The labeled duplex-forming oligonucleotide F10T (5′-*FAM*-dTATAGCTA-HEG-TATAGCTATAT-*TAMRA*-3′) (HEG linker: [$(-CH_2-CH_2-O-)_6$]) was treated in the same manner, except that the buffer was changed to 10 mM lithium cacodylate (pH 7.4). Fluorescence readings were taken at intervals of 0.5 °C over the range of 25 to 95 °C.

G-quadruplex fluorescent intercalator displacement (G4-FID) assay

The FID assay was performed as previously described.[4] 0.25 μM pre-folded DNA target is mixed with thiazole orange (TO, 0.50 μM for c-kit87 and 0.75 μM for ds26) in Tris-HCl

buffer (10 mM, pH 7.2) containing 100 mM KCl, in a total volume of 3 mL. Each ligand addition is followed by a 3-min equilibration period after which the fluorescence spectrum is recorded. The percentage of displacement is calculated from the fluorescence area (FA, 510–750 nm, excitation, 501 nm).

DNA preparation and IFN-γ detection

The DNA substrate (100 μM) was dissolved in Tris-HCl buffer (10 mM, pH 7.2). The solution was heated to 95 °C for 10 min and then cooled at 0.1 °C/s to room temperature to allow the formation of the hairpin structure. The annealed product was stored at –20 °C before use. For IFN-γ detection, 0.7 μL of the DNA substrate in Tris-HCl buffer (10 mM, pH 7.2) was diluted into 10 μL binding buffer (10 mM Hepes, 100 mM KCl, 1 mM EDTA, pH 7.4) by enzyme free water with certain concentration of IFN-γ. After incubation at 37 °C for 5 min, the samples were diluted to 100 μL with Tris-HCl buffer (10 mM, 50 mM KCl, pH 7.2) and then incubated at room temperature for 60 min. The mixture was diluted using Tris-HCl buffer (10 mM, pH 7.2) to a final volume of 500 μL. Finally, 1.0 μM of complex **8** was added to the mixture. Emission spectra were recorded in the 460–740 nm range using an excitation wavelength of 317 nm.

Synthesis

The complexes was prepared according to (modified) literature methods.[5] All complexes are characterized by ^{1}H-NMR, ^{13}C-NMR, high resolution mass spectrometry (HRMS) and elemental analysis. The precursor iridium(III) complex dimer $[Ir_2(C\hat{}N)_4Cl_2]$ is prepared as reported method.[6] Then, a suspension of $[Ir_2(C\hat{}N)_4Cl_2]$ (0.2 mmol) and corresponding N^N ligands (0.44 mmol) in a mixture of DCM:methanol (1:1, 20 mL) was refluxed overnight

under a nitrogen atmosphere. The resulting solution was then allowed to cool to room temperature, and filtered to remove unreacted cyclometallated dimer. To the filtrate, an aqueous solution of ammonium hexafluorophosphate (excess) was added and the filtrate was reduced in volume by rotary evaoration until precipitation of the crude product occurred. The precipiate was then filtered and washed with several portions of water (2 × 50 mL) followed by diethyl ether (2 × 50 mL). The product was recrystallized by acetonitrile:diethyl ether vapor diffusion to yield the titled compound.

Complex **1**. Reported.[7]

Complex **2**. Reported.[7]

Complex **3**. Reported.[7]

Complex **4**. Reported.[7]

Complex **5**. Reported.[7]

Complex **6**. Reported.[8]

Complex **7**. Reported.[7]

Complex **8**. Yield: 50%. ^{1}H NMR (400 MHz, Acetonitrile-d_3) δ 8.48 (d, J = 1.6 Hz, 2H), 8.06-8.04 (m, 4H), 7.95 (dd, J = 8.0, 0.8 Hz, 2H), 7.62 (dd, J = 7.6, 2.0 Hz, 2H), 7.42 (d, J = 0.8 Hz, 2H), 7.14-7.12 (m, 4H), 6.94-6.90 (m, 2H), 6.43 (d, J = 7.6 Hz, 2H), 6.09 (d, J = 8.4 Hz, 2H), 1.43 (s, 18H); ^{13}C NMR (100 MHz, Acetonitrile-d_3) δ 181.2, 164.4, 156.0, 150.8, 150.4, 148.9, 140.1, 132.8, 131.6, 131.4, 127.5, 126.4, 125.7, 125.3, 123.6, 122.8, 121.5, 35.2, 29.1; MALDI-TOF-HRMS: Calcd. for $C_{44}H_{40}IrN_4S_2[M–PF_6]^+$: 881.2324 found: 881.2326; Anal.: ($C_{44}H_{40}IrN_4S_2$ PF_6) C, H, N: calcd. 51.50, 3.93, 5.46; found 51.21, 4.10, 5.52.

Complex **9**. Reported.[9]

Structure-activity relationship of the iridium(III) complexes

Preliminary structure-activity relationships can be derived from comparing the DNA-binding behaviors of these iridium(III) complexes. Since complexes **1**, **2** and **7** all possess the same

pbtz C^N ligand, the superior G-quadruplex-selectivity of complex **8** could be due to the dtbpy N^N ligand that it carries. Interestingly, although the N^N ligands of complexes **1**, **5** and **8** all share the same basic 2,2'-bipyridine (bpy) framework, the superior performance of **8** suggests that the t-butyl substituents at the 4 and 4' positions of the bpy scaffold are important for G-quadruplex affinity, possibly due to their ability to facilitate additional contact interactions with the loop or groove regions of the G-quadruplex.[10] Among the complexes in the focused library, although **9** bears the same dtbpy N^N ligand as **8**, its lower G-quadruplex-binding selectivity suggests that the pbtz C^N ligand of **8** is superior to the 2-phenylpyridine C^N ligand carried by complex **9**.

Table S1. Photophysical properties of iridium(III) complexes **1**–**9**.

Complex	Quantum yield	λ_{em} [nm]	Lifetime [μs]	UV/vis absorption λ_{abs} (ε) [nm] ([$dm^3 \cdot mol^{-1} \cdot cm^{-1}$])
1	0.431	526	$4.826 \pm 4.869 \times 10^{-3}$	321 (2.59×10^4), 414 (5.20×10^3)
2	0.554	532	$4.837 \pm 5.246 \times 10^{-3}$	284 (4.08×10^4)
3	0.384	560	$4.829 \pm 4.987 \times 10^{-3}$	258 (4.70×10^4), 332 (2.08×10^4), 438 (4.30×10^3)
4	0.671	558	$4.539 \pm 6.148 \times 10^{-3}$	258 (3.84×10^4), 438 (2.40×10^3)
5	0.098	588	$4.772 \pm 6.490 \times 10^{-3}$	289 (3.46×10^4), 334 (1.64×10^4), 438 (5.60×10^3)
6	0.269	556	$4.851 \pm 5.753 \times 10^{-3}$	212 (6.52×10^4), 250 (3.92×10^4), 315 (1.72×10^4), 415 (1.40×10^3)
7	0.162	585	$4.667 \pm 4.529 \times 10^{-3}$	272 (3.78×10^4), 311 (2.61×10^4)
8	0.322	532	$2.943 \pm 4.927 \times 10^{-2}$	292 (4.90×10^4), 307 (5.04×10^4), 320 (4.57×10^4), 412 (1.19×10^4)
9	0.233	581	$0.603 \pm 5.530 \times 10^{-2}$	267 (3.07×10^4), 313 (1.40×10^4), 337 (7.90×10^3)

Table S2 Comparison of IFN-γ detection assays reported in recent years.

Method	Detection limit	Dynamic detection range (linear range)	Interference sample test
Dextran-coated surface plasmon resonance sensor[11]	[a] 250 $ng \cdot mL^{-1}$ (about 14.97 nM)	250–1000 $ng \cdot mL^{-1}$ (*)	1% human serum
Aptamer-based electrochemical sensor[12]	1 pM (for DNA aptamer)	1–1 × 10^6 pM (*)	*
Fluorescence resonance energy transfer-based aptamer beacon[13]	5 nM	1–100 nM (5–100 nM)	RPMI1640 media with 10% fetal bovine serum
Antibody-based surface plasmon resonance sensor[14]	[a] 50 $ng \cdot mL^{-1}$ (about 2.99 nM)	50–1000 $ng \cdot mL^{-1}$ (*)	RPMI1640 media with 10% fetal bovine serum
Aptamer-based electrochemical biosensor[15]	0.06 nM	0.06–40 nM (0.06–10 nM)	*
Aptamer-based surface micropatterning[16]	5 nM	1–100 nM (5–100 nM)	*
Functional DNA magnetic beads and personal glucose meter[17]	2.6 nM	0–400 nM (*)	20% human serum
Engineered protein-based surface plasmon resonance biosensor[18]	1 nM	1–100 nM (*)	22% human plasma

Electrochemical DNA biosensor based on hybridization chain reaction with enzyme-amplification[19]	0.3 nM	0–600 nM (0.5–300 nM)	RPMI1640 media with 10% fetal bovine serum
Aptamer-based surface plasmon resonance immunosensor[20]	33 pM	0.3–333 nM (0–10 nM)	10% human plasma
Engineered protein-based surface plasmon resonance biosensor[21]	0.2 nM	2–500 nM (*)	albumin-depleted 2% human plasma
DNAzyme-based electrochemical aptasensor[22]	0.1 nM	0–120 nM (*)	*
Graphene and DNase I-based electrochemical aptasensor[23]	0.065 pM	0–1 nM (0.1–0.7 pM)	RPMI1640 media with 10% fetal bovine serum

[a] The lowest detectable concentration.

* Not mentioned in the reference.

Fig. S1 (a) Diagrammatic bar array representation of the luminescence enhancement selectivity ratio of complexes **1**–**6** for c-kit87 G-quadruplex DNA over dsDNA (ds26) and ssDNA. (b) Diagrammatic bar array representation of the luminescence enhancement selectivity ratio of complexes **2**, **7**–**9** for c-kit87 G-quadruplex DNA over dsDNA (ds26) and ssDNA. The concentration of complexes **1**–**9** was 1.0 μM, the concentration of DNA was 5 μM.

(a)

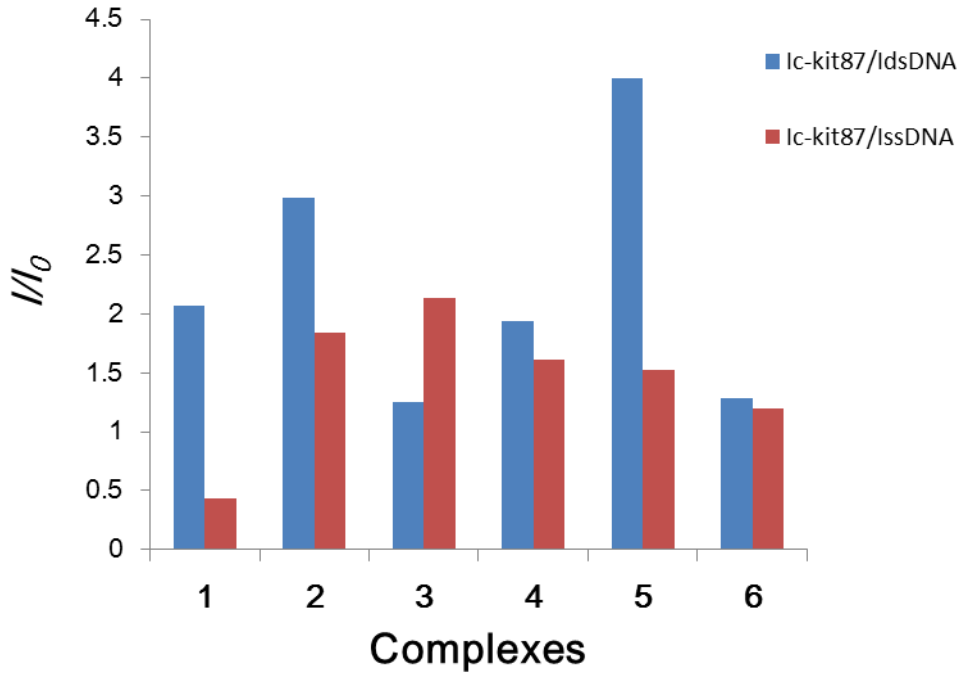

(b)

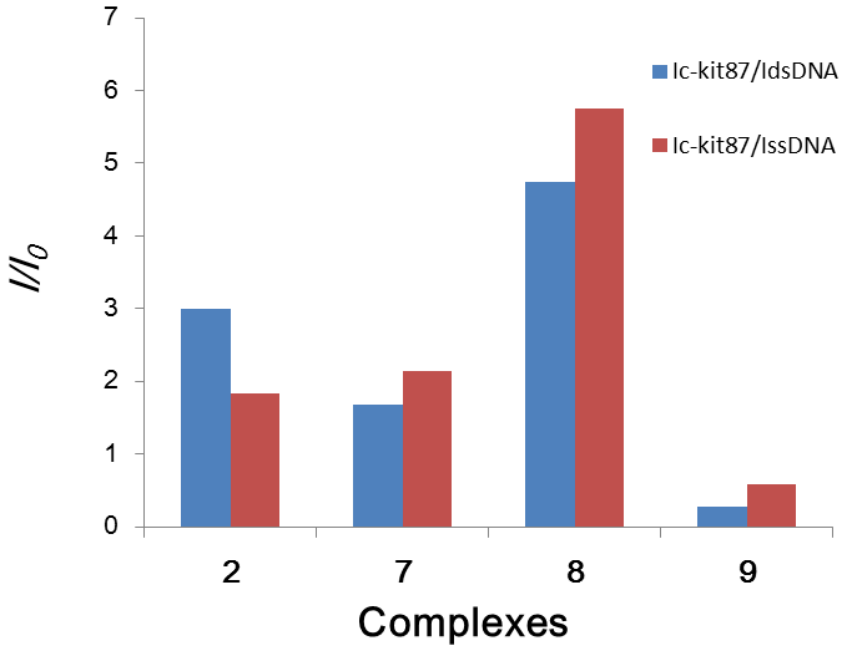

Fig. S2 Emission spectrum of complex **8** (1.0 μM) in the presence of 5 μM of CCR5, ct-DNA or various G-quadruplexes.

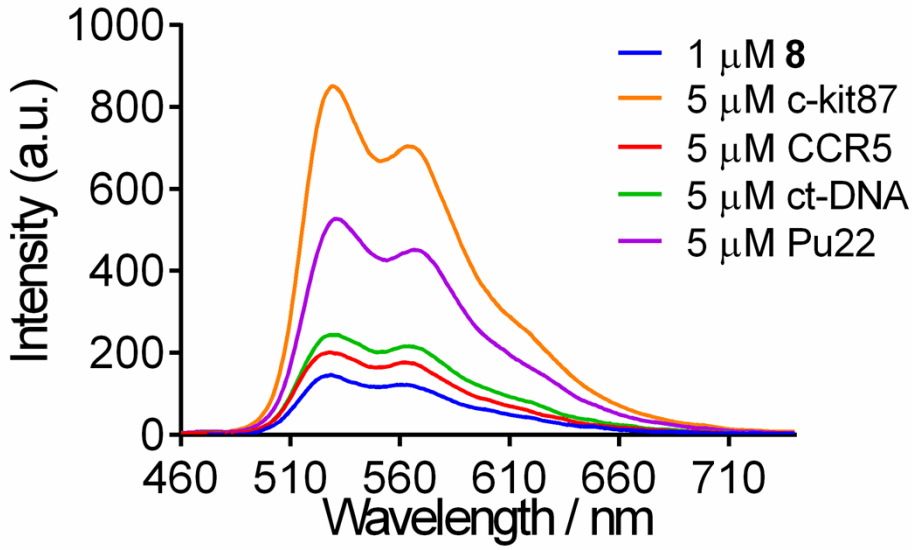

Fig. S3 Competitive FRET-melting assay results for complex **8** (3 μM) in the presence of G-quadruplexes (1 μM) with different loop lengths at (a) 5'-side loop, (b) central loop or (c) 3'-side loop as the competitor. The decrease in melting temperature is shown as a function of loop size.

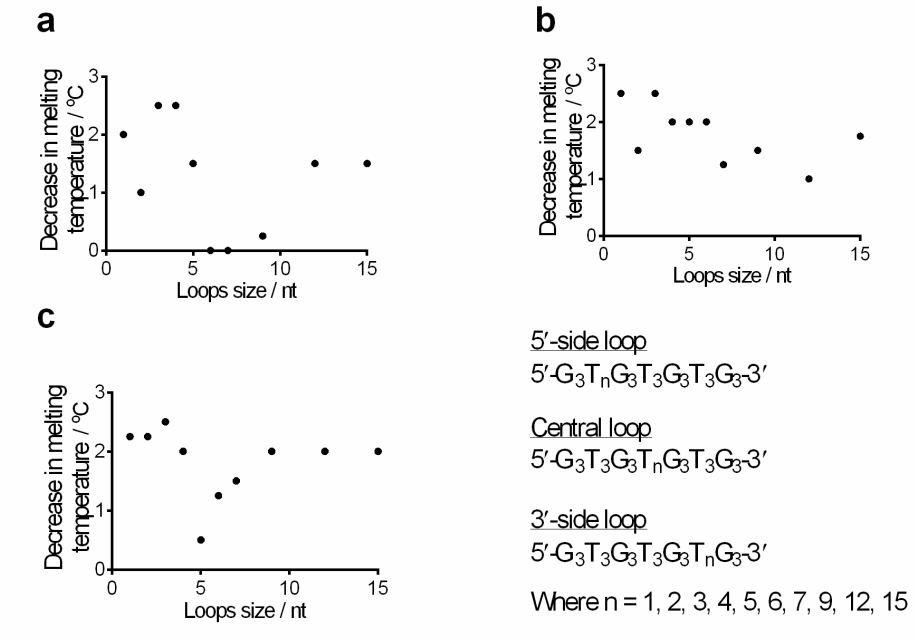

Fig. S4 (a) Relative luminescence intensity of the system with different concentrations of DNA (0.04, 0.06, 0.10, 0.14, 0.20, 0.30 and 0.40 μM). (b) Relative luminescence intensity of the system with different concentrations of **8** (0.3, 0.5, 0.7, 1.0 and 1.5 μM). (c) Relative luminescence intensity with different incubation temperatures (23, 30, 37 and 45 ºC). (d) Relative luminescence intensity with different incubation times (15, 20, 25, 30, 40, 50, 60 and 75 min). Unless otherwise stated, the concentration of complex **8** was 1.0 μM, the concentration of DNA was 0.14 μM, and Tris buffer (10 mM Tris, pH 7.2) was used.

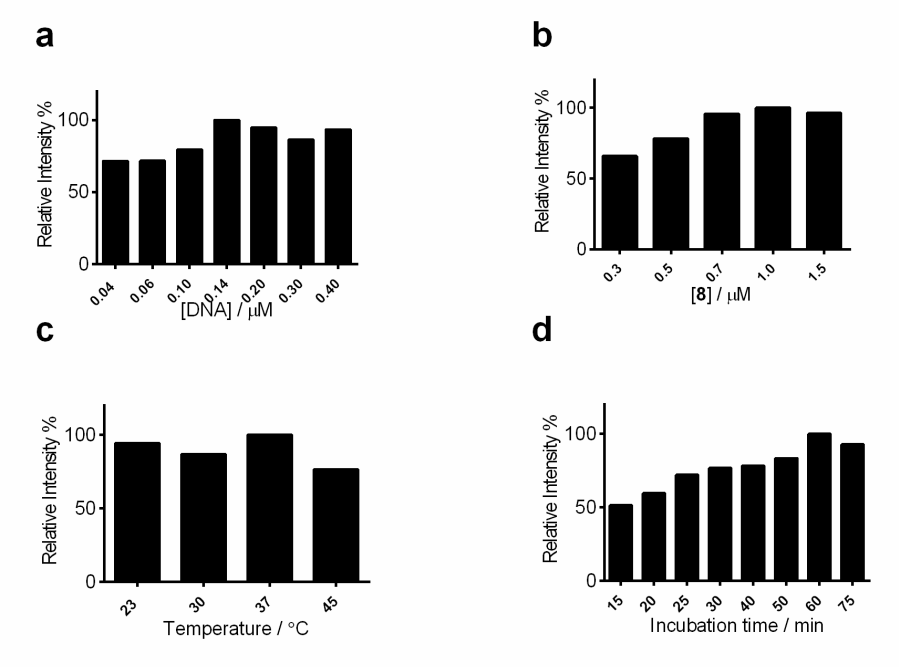

Fig. S5 UV/Vis spectrophotometric titration of 20 μM complex **8** with increasing concentrations of c-kit87 (0, 0.2, 0.6, 1.0, 1.4 and 1.8 μM).

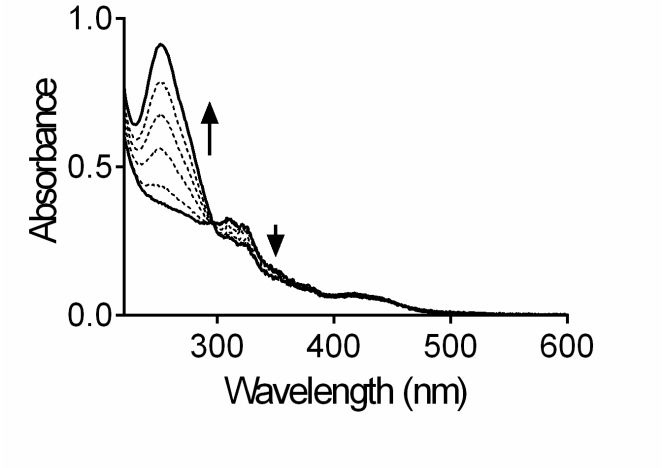

References

1 H. Yu, X. Wang, M. Fu, J. Ren and X. Qu, *Nucleic Acids Res.*, 2008, **36**, 5695.
2 H.-Z. He, D. S.-H. Chan, C.-H. Leung and D.-L. Ma, *Chem. Commun.*, 2012, **48**, 9462.
3 G. A. Crosby and J. N. Demas, *J. Phys. Chem.*, 1971, **75**, 991.
4 D. Monchaud, C. Allain, H. Bertrand, N. Smargiasso, F. Rosu, V. Gabelica, A. De Cian, J. L. Mergny and M. P. Teulade-Fichou, *Biochimie*, 2008, **90**, 1207.
5 D.-L. Ma, L.-J. Liu, K.-H. Leung, Y.-T. Chen, H.-J. Zhong, D. S.-H. Chan, H.-M. D. Wang and C.-H. Leung, *Angew. Chem. Int. Ed.*, 2014, **53**, 9178.
6 Q. Zhao, S. Liu, M. Shi, C. Wang, M. Yu, L. Li, F. Li, T. Yi and C. Huang, *Inorg. Chem.*, 2006, **45**, 6152.
7 S. Lin, W. Gao, Z. Tian, C. Yang, L. Lu, J.-L. Mergny, C.-H. Leung and D.-L. Ma, *Chem. Sci.*, 2015, **6**, 4284.
8 K.-H. Leung, H.-Z. He, B. He, H.-J. Zhong, S. Lin, Y.-T. Wang, D.-L. Ma and C.-H. Leung, *Chem. Sci.*, 2015, **6**, 2166.
9 J. D. Slinker, A. A. Gorodetsky, M. S. Lowry, J. Wang, S. Parker, R. Rohl, S. Bernhard and G. G. Malliaras, *J. Am. Chem. Soc*, 2004, **126**, 2763.
10 M.-Y. Kim, H. Vankayalapati, K. Shin-ya, K. Wierzba and L. H. Hurley, *J. Am. Chem. Soc.*, 2002, **124**, 2098.
11 E. C. A. Stigter, G. J. d. Jong and W. P. van Bennekom, *Biosens. Bioelectron.*, 2005, **21**, 474.
12 K. Min, M. Cho, S.-Y. Han, Y.-B. Shim, J. Ku and C. Ban, *Biosens. Bioelectron.*, 2008, **23**, 1819.
13 N. Tuleuova, C. N. Jones, J. Yan, E. Ramanculov, Y. Yokobayashi and A. Revzin, *Anal. Chem.*, 2010, **82**, 1851.
14 G. Stybayeva, M. Kairova, E. Ramanculov, A. L. Simonian and A. Revzin, *Colloids Surf., B*, 2010, **80**, 251.
15 Y. Liu, N. Tuleouva, E. Ramanculov and A. Revzin, *Anal. Chem.*, 2010, **82**, 8131.
16 N. Tuleuova and A. Revzin, *Cel. Mol. Bioeng.*, 2010, **3**, 337.
17 Y. Xiang and Y. Lu, *Nat. Chem.*, 2011, **3**, 697.
18 H. Šípová, V. Ševců, M. Kuchař, J. N. Ahmad, P. Mikulecký, P. Šebo, P. Malý and J. Homola, *Procedia Engineer.*, 2011, **25**, 940.
19 J. Zhao, C. Chen, L. Zhang, J. Jiang and R. Yu, *Biosens. Bioelectron.*, 2012, **36**, 129.
20 C.-C. Chang, S. Lin, C.-H. Lee, T.-L. Chuang, P.-R. Hsueh, H.-C. Lai and C.-W. Lin, *Biosens. Bioelectron.*, 2012, **37**, 68.
21 H. Šípová, V. Ševců, M. Kuchař, J. N. Ahmad, P. Mikulecký, R. Osička, P. Malý and J. Homola, *Sens. Actuator B*, 2012, **174**, 306.
22 H. Zhang, B. Jiang, Y. Xiang, Y. Chai and R. Yuan, *Analyst*, 2012, **137**, 1020.
23 G. Yan, Y. Wang, X. He, K. Wang, J. Liu and Y. Du, *Biosens. Bioelectron.*, 2013, **44**, 57.